Neuron
Article

Extracellular Interactions between GluR2 and N-Cadherin in Spine Regulation

Laura Saglietti,[1] Caroline Dequidt,[2] Kinga Kamieniarz,[1,6] Marie-Claude Rousset,[3] Pamela Valnegri,[1] Olivier Thoumine,[2] Francesca Beretta,[1] Laurent Fagni,[3] Daniel Choquet,[2] Carlo Sala,[4] Morgan Sheng,[5] and Maria Passafaro[1,*]

[1] DTI Dulbecco Telethon Institute, CNR Institute of Neuroscience, Cellular and Molecular Pharmacology, Department of Pharmacology, University of Milan, Italy
[2] CNRS, UMR 5091, Institute Magendie de Neurosciences, Universitè Bordeaux, France
[3] Institut de Génomique Fonctionnelle, Unité Mixte de Recherche 5203, 34000 Montpellier, France
[4] CNR Institute of Neuroscience, Cellular and Molecular Pharmacology, Department of Pharmacology, University of Milan, Italy
[5] The Picower Institute for Learning and Memory, RIKEN-MIT Neuroscience Research Center, Howard Hughes Medical Institute, Massachusetts Institute of Technology, Cambridge, MA 02139, USA
[6] Present address: Department of Molecular Virology, Institute of Experimental Biology, Umultowska, Poznan, Poland.
*Correspondence: m.passafaro@in.cnr.it
DOI 10.1016/j.neuron.2007.04.012

SUMMARY

Via its extracellular N-terminal domain (NTD), the AMPA receptor subunit GluR2 promotes the formation and growth of dendritic spines in cultured hippocampal neurons. Here we show that the first N-terminal 92 amino acids of the extracellular domain are necessary and sufficient for GluR2′s spine-promoting activity. Moreover, overexpression of this extracellular domain increases the frequency of miniature excitatory postsynaptic currents (mEPSCs). Biochemically, the NTD of GluR2 can interact directly with the cell adhesion molecule N-cadherin, in *cis* or in *trans*. N-cadherin-coated beads recruit GluR2 on the surface of hippocampal neurons, and N-cadherin immobilization decreases GluR2 lateral diffusion on the neuronal surface. RNAi knockdown of N-cadherin prevents the enhancing effect of GluR2 on spine morphogenesis and mEPSC frequency. Our data indicate that in hippocampal neurons N-cadherin and GluR2 form a synaptic complex that stimulates presynaptic development and function as well as promoting dendritic spine formation.

INTRODUCTION

α-Amino-3-hydroxy-5-methylisoxazolepropionate (AMPA) receptors are ionotropic glutamate receptors that mediate the majority of excitatory synaptic transmission in the mammalian central nervous system (CNS) (Dingledine et al., 1999). Changes in the number of postsynaptic AMPA receptors contribute to long-lasting changes in synaptic strength, including long-term potentiation (LTP) and long-term depression (LTD) (Malinow and Malenka, 2002) and dendritic spine enlargement (Kopec et al., 2006). AMPA receptors are tetrameric complexes composed of up to four distinct subunits, of which GluR1, GluR2, and GluR3 predominate in mature hippocampal neurons (Wenthold et al., 1996). Each GluR subunit contains an extracellular NTD (also known as amino terminal domain [ATD]; residues 60–398 in GluR2), a ligand-binding domain, four hydrophobic domains of which M1, M3, and M4 traverse the membrane, and an intracellular carboxy-terminal tail (Wollmuth and Sobolevsky, 2004).

The NTD shows sequence homology to the bacterial periplasmic amino acid-binding protein LIVBP (leucine, isoleucine, valine-binding protein) (Masuko et al., 1999; O'Hara et al., 1993; Paoletti et al., 2000) and to the extracellular (ligand-binding) domain of metabotropic glutamate receptors (mGluRs) (Armstrong et al., 1998; Stern-Bach et al., 1994). One function of the NTD of AMPA receptors is to specify the initial assembly of GluR subunits into dimers (Ayalon and Stern-Bach, 2001). Recently, we found that overexpression of specifically the GluR2 subunit promotes spine growth in cultured neurons and that this activity requires the NTD of GluR2 (Passafaro et al., 2003). Moreover, RNAi knockdown of GluR2 inhibits spine morphogenesis.

Dendritic spines are small protrusions on dendritic shafts that constitute the postsynaptic contact sites for the majority of excitatory synapses in the mammalian central nervous system (Harris and Kater, 1994; Hering and Sheng, 2001). Spines are heterogeneous in shape and size, and their density and morphology are influenced by many factors, including age and hormonal status (Harris, 1999; Hering and Sheng, 2001; Nimchinsky et al., 2002). Although their function remains unclear, dendritic spines are considered to play critical roles in the regulation of synaptic transmission in normal and pathological conditions (Fiala et al., 2002; Nimchinsky et al., 2002).

Classic cadherins are single-pass transmembrane proteins with five ectodomain repeats (EC1-EC5 domains) that are separated by calcium-binding sites, and a short intracellular domain that is conserved between family members. The N-terminal domain mediates the homophilic

adhesion, while the c-terminal tail binds α- and β-catenins and anchors the cadherin complex to the actin cytoskeleton (Bamji, 2005; Boggon et al., 2002; Pertz et al., 1999). Some structural and functional data indicate that the most membrane-distal EC domain (EC1) is important for both adhesion and recognition (Boggon et al., 2002; Nose et al., 1990; Shapiro et al., 1995; Tamura et al., 1998), while other work suggests that all of the EC domains participate in the adhesive interface (Chappuis-Flament et al., 2001). However, it is generally agreed that multiple *trans* interactions between cadherin proteins on adjacent cells cooperate in generating strong intercellular adhesion (Boggon et al., 2002; Gumbiner, 2005; Yap et al., 1997). Lateral (*cis*) interactions between cadherins are regulated by proteins binding to juxtamembrane domain (Yap et al., 1997), while the principal link to actin occurs over an extended portion of the C-tail where β-catenin binds to cadherin and to α-catenin, which in turn binds directly to actin (Elste and Benson, 2006). Cadherins and their associated proteins have been observed in many neuronal populations in CNS (Salinas and Price, 2005). The expression and subcellular distribuition of cadherins vary with the type and developmental stage of a synapse (Salinas and Price, 2005). The most prominent cadherin in neurons, N-cadherin, is known to be important for pre- and postsynaptic adhesion. N-cadherin plays a key role during synaptogenesis, neurite outgrowth, dendrite arborization, and axon guidance (Benson and Tanaka, 1998; Nakai and Kamiguchi, 2002; Yu and Malenka, 2003). During later stages of development, N-cadherin is concentrated at synapses (Beesley et al., 1995; Uchida et al., 1996), where it is involved in the regulation of synaptic adhesion, function, and plasticity (Bozdagi et al., 2000; Murase et al., 2002; Okamura et al., 2004; Tanaka et al., 2000; Togashi et al., 2002). N-cadherin and its interaction with catenins is essential for proper development of dendritic spines (Takeichi and Abe, 2005).

Here we investigate the molecular basis of GluR2′s ability to promote spine growth and enlargement. Unexpectedly, we find that the NTD of GluR2 (but not GluR1) mediates a specific and direct interaction with N-cadherin, an extracellular interaction that can occur in *cis* or in *trans* membranes. Moreover, RNAi experiments show that N-cadherin is required for the effect of GluR2-NTD overexpression on spine growth. Our results suggest that N-cadherin and GluR2 form a synaptic complex that stimulates synaptic function and promotes dendritic spine growth and formation.

RESULTS

NTD of GluR2 Is Sufficient to Induce Spine Enlargement and Affect Synaptic Activity

To test the role of GluR2′s NTD in spine growth, we constructed a series of chimeras in which the NTD of GluR2 was fused to the transmembrane domain of unrelated membrane proteins: pDisplay (containing a transmembrane region of PDGF receptor) or CD4 (a T-lymphocyte surface protein) (Maddon et al., 1985), giving rise to NTDR2-pDisplay and NTDR2-CD4 (Figure 1A). Overexpression of NTDR2-CD4 or NTDR2-pDisplay chimeras in mature cultured hippocampal neurons (22 days in vitro [DIV22]; visualized by cotransfected enhanced green fluorescent protein [EGFP]) caused an increase in spine length and an enlargement of spine heads compared to neurons transfected with EGFP alone (Figures 1A and 1C and Table 1). In younger neurons (DIV11), NTDR2-pDisplay or NTDR2-CD4 overexpression induced an increase in the length and density of filopodia-like protrusions compared to control (Table 1). In cumulative frequency plots, neurons overexpressing NTDR2-pDisplay or NTDR2-CD4 showed a roughly parallel rightward shift in spine diameter and length (Figure 1C). The density of spines was also increased ∼1.5- and ∼1.7-fold by overexpression of NTDR2-pDisplay and NTDR2-CD4, respectively (Figure 1D and Table 1). By contrast, overexpression of NTDR1-pDisplay (NTD from GluR1 fused to pDisplay) reduced the length and width of spines (Figures 1A–1C and Table 1), while overexpression of NTDR1-CD4 had no effect on the width but reduced the length of dendritic spines (Figures 1A–1C and Table 1). Thus, the extracellular NTD of GluR2 is sufficient to enhance spine density and growth when fused to a heterologous transmembrane protein.

Furthermore, we examined the staining of endogenous pre- and postsynaptic markers. In neurons overexpressing GluR2-NTD, but not GluR1-NTD, there was a significant increase in the number of puncta for synaptophysin (1.5 ± 0.11 relative to control, $p < 0.01$), bassoon (1.3 ± 0.12 relative to control, $p < 0.05$), shank (1.6 ± 0.13 relative to control, $p < 0.01$), and N-cadherin (1.6 ± 0.19 relative to control, $p < 0.05$) (Figures 2A and 2B). We also found that spines of GluR2-NTD-overexpressing cells showed increased staining intensity for synaptophysin (2.5 ± 0.12 relative to control, $p < 0.01$), shank (1.8 ± 0.21 relative to control, $p < 0.01$), bassoon (2.1 ± 0.18 relative to control, $p < 0.05$), and N-cadherin (2.5 ± 0.24 relative to control, $p < 0.01$), consistent with the expansion of spine head and synapse (Figures 2A–2C).

Given the morphological and molecular changes induced by NTDR2-pDisplay overexpression, we explored functional effects by recording spontaneous miniature EPSCs (mEPSCs) in cultured hippocampal neurons. Frequency of AMPA receptor-mediated mEPSCs increased greatly in neurons transfected with NTDR2-pDisplay, but not NTDR1-pDisplay (Figures 3A and 3B). The amplitude of mEPSCs was not significantly affected either by NTDR2-pDisplay or by NTDR1-pDisplay. Since changes in mEPSC frequency generally reflect altered number of synapses or presynaptic release probability, we used FM1-43 dye uptake to evaluate the number of functional presynaptic terminals contacting transfected neurons. Indeed, GluR2-NTDR2 overexpression was associated with a marked increase in FM1-43 staining density associated with the transfected neurons (2.1 ± 0.01 relative to control neurons transfected with DsRed, $p < 0.01$), which correlated with the elevated mini frequency (Figures 3A and 3B).

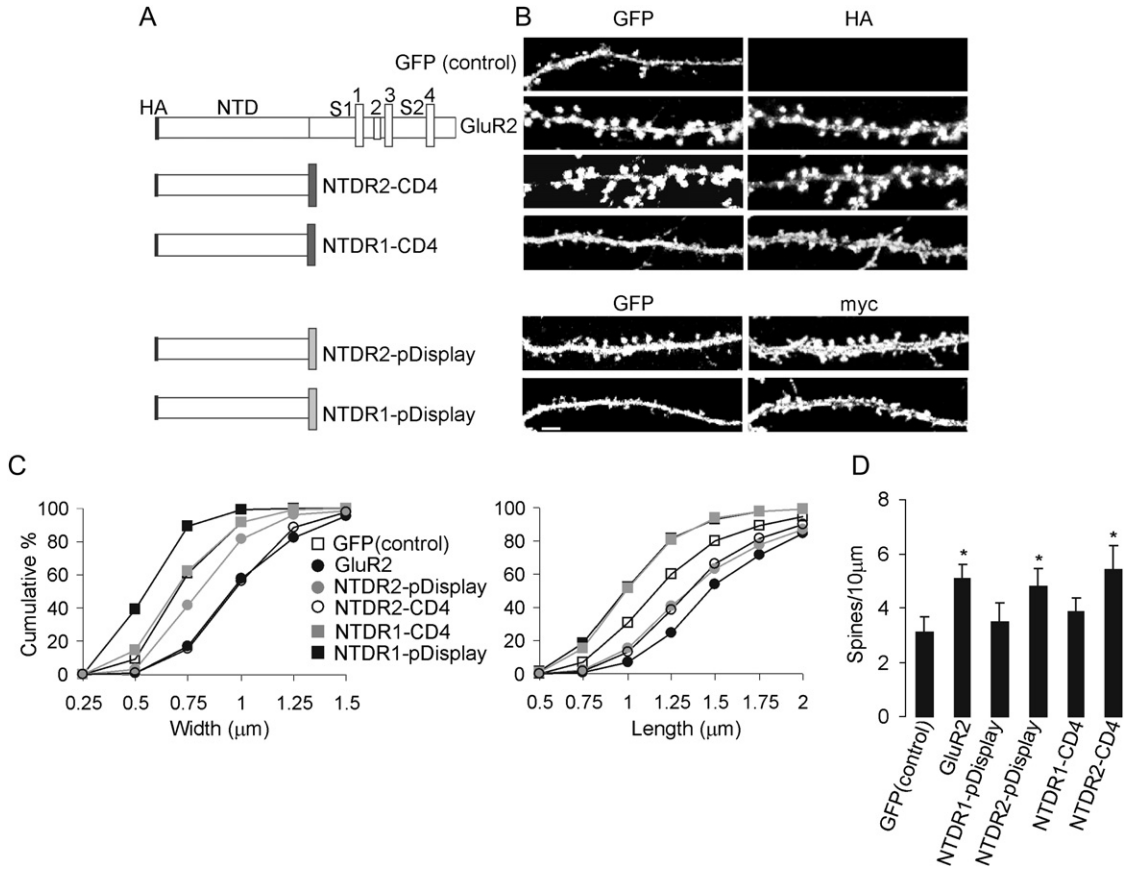

Figure 1. NTDR2 Is Sufficient to Induce Spine Modifications in Hippocampal Neurons

(A) Diagram of chimeric constructs between NTD GluRs and pDisplay or CD4.

(B) The hippocampal neurons were transfected with EGFP alone (control) or with EGFP and NTD chimeras, as indicated at left. Each pair of images shows the transfected chimeric construct stained by HA or Myc (right) and cotransfected EGFP fluorescence to outline dendrite/spine morphology (left). Scale bars, 2.5 μm (high magnification).

(C) Cumulative frequency plots of spine length (μm) and spine head width (μm) in neurons transfected as in (B) (>1000 spines and >18 neurons examined for each construct).

(D) Quantification of spine density (number of spines per 10 μm of dendrite length) in neurons transfected as in (B) (>16 neurons examined for each construct). Histograms show mean values ± SEM.

These findings indicate that overexpression of membrane-attached NTDR2, but not NTDR1, is sufficient to increase the number of functionally detectable AMPA receptor-containing synapses and to induce an enhancement in presynaptic function (or increased number of functional presynaptic contacts) onto the transfected cell. Together these results show that the NTD of GluR2 stimulates presynaptic development and function as well as dendritic spine formation. Since the NTD is an extracellular domain, it could achieve this effect by interaction with a surface protein of the postsynaptic or presynaptic membrane.

N-Terminal 92 Amino Acids of the Extracellular Domain Are Essential for GluR2's Spine-Promoting Activity

To narrow down the region within the NTD of GluR2 responsible for its spine-promoting effects, we made chimeric swaps between the NTDs of GluR1 and GluR2 using as boundary two small regions conserved in both subunits (GVYAIFGFV, ending at residue 92 for GluR2 and at 87 for GluR1; and LFQDLE, ending at residue 199 for GluR2 and 190 for GluR1). The chimera GluR2(199)R1 (obtained by replacing the first 190 amino acids of GluR1 with the first 199 aa of GluR2) induced an increase in spine length and spine head width compared to neurons transfected with GFP alone (Figures 4A–4C and Table 1). GluR2(92)R1 (obtained by replacing the first 87 amino acids of GluR1 with the first 92 aa of GluR2) also increased spine dimensions (Figures 4A–4C). Spine density was also significantly enhanced by GluR2(92)R1 and GluR2(199)R1 (Figure 2D). Deletion of the first 92 aa (Δ92GluR2) abolished the spine-promoting activity of GluR2-NTD (Figures 4B and 4C and Table 1).

The converse chimeras in which the NTD of GluR2 is partly replaced with the NTD of GluR1 [GluR1(87)R2 and GluR1(190)R2] had no effect on spine morphology

Table 1. Dendritic Spine Size and Density (Mean ± SEM) in Neurons Transfected with GluR Constructs

Age of Culture	Transfected/Treated with	Length of Spine (μm)	Width of Spine Head (μm)	Number of Spines/10 μm
DIV22	GFP (control)	1.26 (±0.14)	0.73 (±0.06)	3.09 (±0.56)
DIV22	GFP + HA-GluR2	1.67 (±0.21)[c]	1.04 (±0.11)[c]	5.10 (±0.48)[c]
DIV22	GFP + NTDR2-pDisplay	1.45 (±0.19)[c]	0.83 (±0.06)[b]	4.8 (±0.66)[c]
DIV22	GFP + NTDR1-pDisplay	1.03 (±0.09)	0.57 (±0.07)	3.5 (±0.71)
DIV22	GFP + NTDR2-CD4	1.43 (±0.10)[c]	0.98 (±0.10)[c]	5.4 (±0.90)[c]
DIV22	GFP + NTDR1-CD4	1.02 (±0.13)	0.68 (±0.11)[a]	3.85 (±0.51)
DIV22	GFP + GluR1(87)R2	1.08 (±0.05)[c]	0.66 (±0.01)[a]	3.27 (±0.6)
DIV22	GFP + GluR2(92)R1	1.41 (±0.09)[b]	0.99 (±0.10)[c]	4.7 (±0.9)[b]
DIV22	GFP + GluR1(190)R2	1.00 (±0.11)[c]	0.64 (±0.06)[a]	3.8 (±0.5)
DIV22	GFP + GluR2(199)R1	1.54 (±0.15)[c]	0.84 (±0.04)[c]	4.63 (±0.52)[b]
DIV22	GFP + Δ92GluR2	0.98 (±0.07)[c]	0.63 (±0.05)[c]	3.35 (±0.22)
DIV22	GFP + NTDR2-pD (int.)	1.33 (±0.19)	0.89 (±0.16)	2.9 (±0.18)
DIV22	GFP + GluR2(92)R1 (int.)	1.35 (±0.22)	0.90 (±0.19)	2.6 (±0.19)
DIV22	PLL3.7 (control)	1.20 (±0.12)	0.70 (±0.11)	3.5 (±0.12)
DIV22	N-cadhsiRNA	1.19 (±0.10)	0.69 (±0.07)	3.1 (±0.14)
DIV22	siRNA + GluR2(199)R1	1.23 (±0.15)	0.71 (±0.01)	3.3 (±0.34)
DIV22	scramble + GluR2(199)R1	1.50 (±0.19)[c]	0.87 (±0.10)[c]	4.68 (±0.22)[b]
DIV22	siRNA + NTDR2-pDisplay	1.30 (±0.15)	0.75 (±0.20)	3.1 (±0.16)
DIV22	Scramble + NTDR2-pDisplay	1.47 (±0.20)[c]	0.90 (±0.25)[c]	4.7 (±0.20)[b]
DIV11	GFP (control)	1.01 (±0.14)	0.61 (±0.15)	3.0 (±0.16)
DIV11	GFP + HA-GluR2	1.63 (±0.22)[c]	0.72 (±0.20)	5.0 (±0.09)[c]
DIV11	GFP + NTDR2-pDisplay	1.60 (±0.11)[c]	0.69 (±0.18)	4.6 (±0.22)[c]
DIV11	GFP + NTDR2-CD4	1.58 (±0.12)[c]	0.70 (±0.18)	4.9 (±0.20)[c]

[a] $p < 0.05$, cf. control neurons.
[b] $p < 0.01$, cf. control neurons.
[c] $p < 0.001$, cf. control neurons (Student's t test).

and density (Figures 4A–4D). Indeed, GluR1(87)R2, GluR1(190)R2, and Δ92GluR2 seemed to have a dominant-negative effect on spine size and spine density.

Frequency, but not amplitude, of mEPSCs was significantly increased in cultured hippocampal neurons expressing GluR2(199)R1 or GluR2(92)R1 constructs (Figure 4E). These results demonstrate that the N-terminal 92 amino acid region of the NTD is sufficient to promote spine morphogenesis and synaptic function.

GluR2 has been shown to induce spine-like protrusions in GABAergic interneurons that usually lack spines (Passafaro et al., 2003). The NTDR2-CD4 and NTDR2-pDisplay constructs also induced spine-like protrusions in GABAergic neurons, as did GluR2(92)R1 (see Figure S1 in the Supplemental Data available online).

GluR2 and N-Cadherin Are Associated in Neurons

We hypothesized that the NTD of GluR2 is the specific site for an extracellular protein-protein interaction. To seek such interacting partners of endogenous GluR2-NTD, surface proteins of neuron cultures were first crosslinked with DTSSP (a nonpermeant crosslinking reagent) and then examined in two-dimensional (2D) diagonal gel electrophoresis (Chan et al., 1998). The first (horizontal) dimension of electrophoresis was performed under nonreducing conditions, and the second (vertical) dimension of the gel was performed under reducing conditions (see Figure S2A). Proteins that are not crosslinked will have the same mobility in both dimensions and will end up on a diagonal line in the gel. Proteins crosslinked by DTSSP will be reduced into their monomeric components in the second dimension and will therefore appear below the diagonal line (Figure S2A). By Western blot analysis of neurons treated with DTSSP, we found that one band below the diagonal line (~100 kDa) was recognized by anti-GluR2 antibody (Figure S2B). To identify specific proteins associated with GluR2, extracts of DTSSP crosslinked neurons were immunopurified with GluR2 C-terminal antibodies

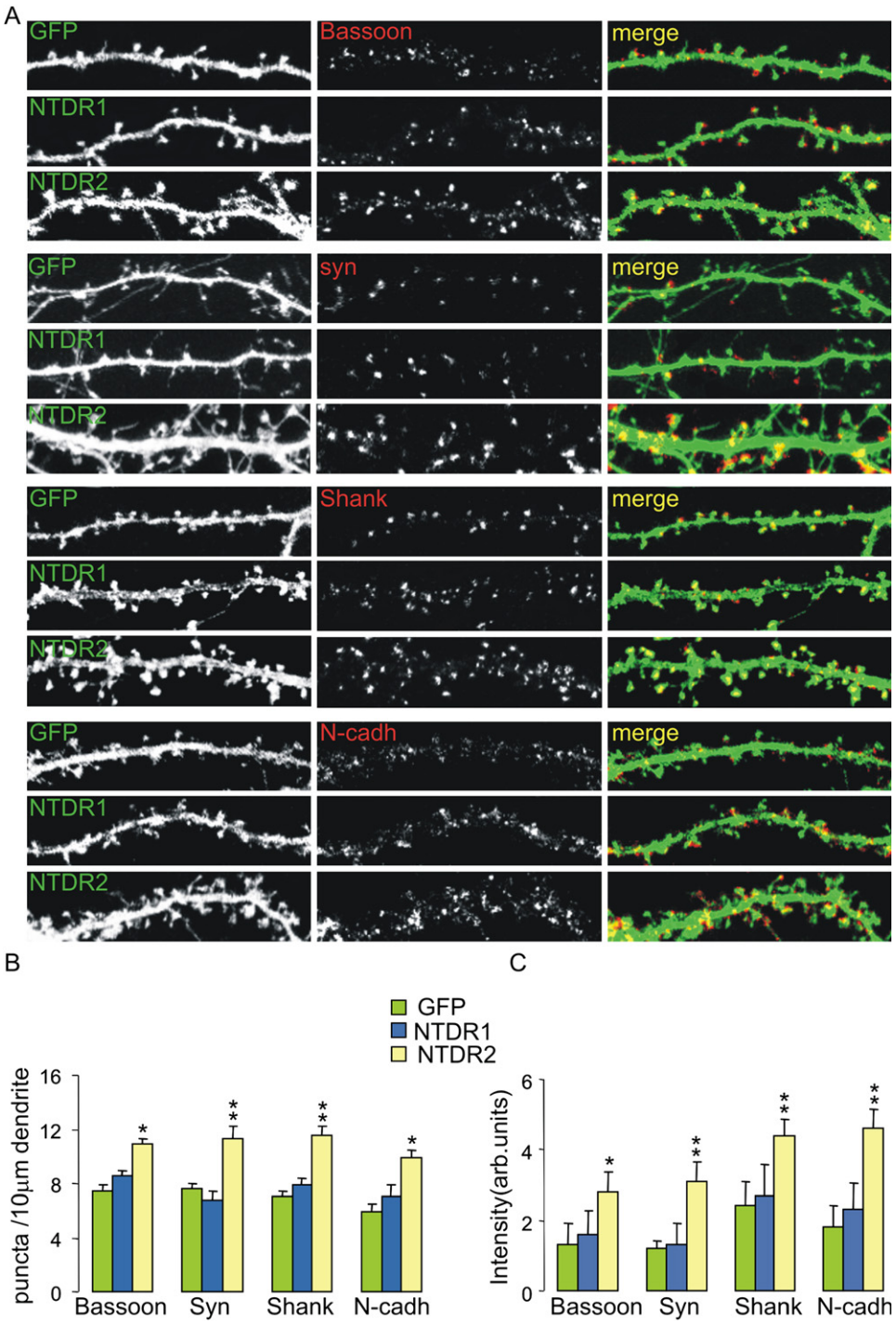

Figure 2. GluR2-NTDR2 Promotes Increased Number of Synapses and Accumulation of Endogenous Synaptic Proteins

(A) Hippocampal neurons at DIV14 were transfected with NTDR2-pDisplay or NTDR1-pDisplay (*myc*-tagged at the N terminus) or with EGFP control and were stained at DIV22. Each row of images shows double labeling for NTDR2 or NTDR1 or GFP (green, left panel) and shank, synaptophysin, bassoon, or N-cadherin (red, middle panel); merge is shown in color in right panel. Individual channels are shown in grayscale.

(B) Quantitation of puncta density of shank, synaptophysin, bassoon, or N-cadherin induced by overexpression of NTDR2-pDisplay (>7 neurons analyzed for each protein; 40 to 70 synapses scored per neuron).

(C) Quantitation of synaptic staining intensity of bassoon, synaptophysin, shank, and N-cadherin induced by overexpression of NTDR2-pDisplay (>7 neurons analyzed for each protein; 40 to 70 synapses scored per neuron). Histograms show mean values ± SEM *p < 0.05, **p < 0.01.

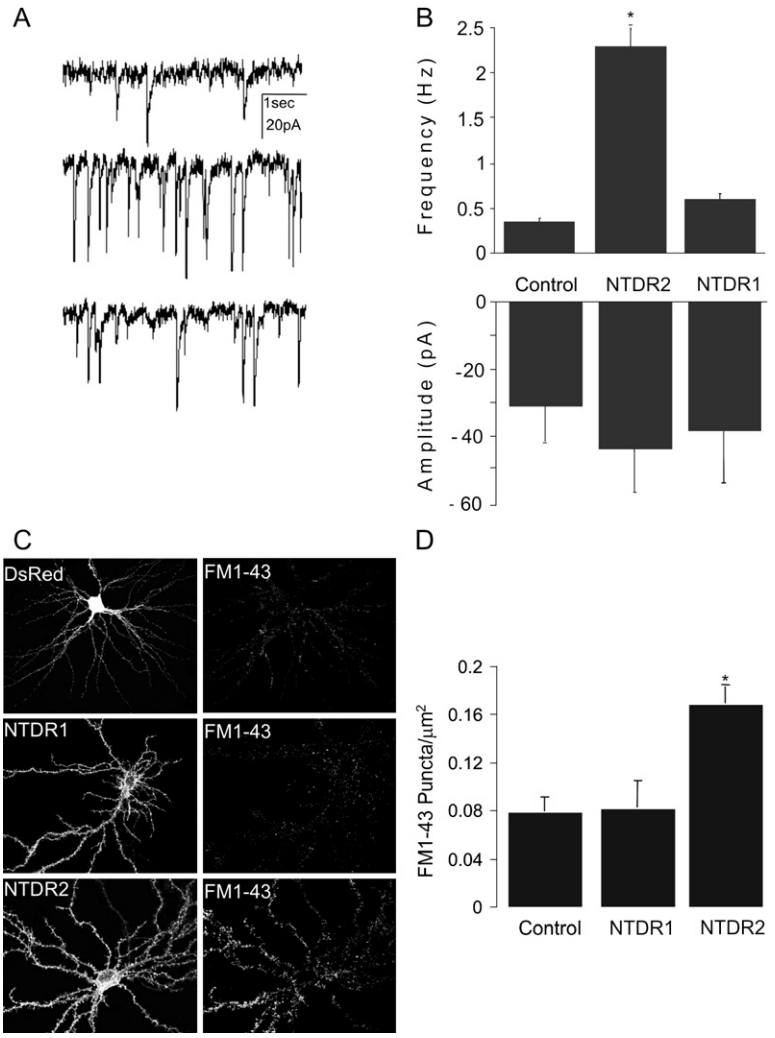

Figure 3. Functional Synaptic Effects of GluR2-NTDR2 Overexpression

NTDR2-pDisplay, but not NTDR1-pDisplay, transgene increased synaptic activity.

(A and B) mEPSCs recorded in control (upper), NTDR2- (middle), and NTDR1-transfected (botton) neurons; histograms show frequency and amplitude (means ± SEM, n = 10) of mEPSCs recorded from control neurons and neurons transfected with NTDR1 or NTDR2-pDisplay at DIV18. * indicates significantly different from control with $p < 0.001$.

(C) FM1-43 staining of functional presynaptic terminals on transfected neurons at DIV18.

(D) Quantitation of puncta density of FM1-43 staining on transfected cells at DIV18. Histograms show mean ± SEM; control with neurons transfected with DsRed. *$p < 0.001$.

and the isolated proteins resolved by diagonal electrophoresis. Silver staining showed a prominent series of bands and spots below the diagonal (Figure 5A, bracket). Mass spectrometry of these spots identified AMPA receptor subunits GluR1, GluR2 at ~100 kDa, stargazin (γ-2) around 50 kDa, and TARP family protein γ-8 in the 50 kDa spot, and N-cadherin in the spot at ~130 kDa (see Table S1). Additional proteins like tubulin, glyceraldehyde dehydrogenase, and HSP90—probable contaminants—were also detected by mass spectrometry (Table S1). Immunoblotting confirmed the presence of GluR2 (Figure 5A) and N-cadherin below the diagonal in the GluR2 immunoprecipitates from surface crosslinked cultures (Figure 5A). These data suggest that AMPA receptor complexes and N-cadherin interact closely on the surface of neurons.

To confirm the association of N-cadherin with GluR2, we performed conventional coimmunoprecipitation studies. From DTTSP surface crosslinked cultures, the GluR2 antibodies were able to coprecipitate N-cadherin as well as stargazin (Figure 5B). We also found GluR1 and β-catenin, but not NR1 and neuroligin-1, in the GluR2 precipitates (Figure 5B). In noncrosslinked samples, coimmunoprecipitation of N-cadherin with GluR2 was greatly diminished (Figure 5B), whereas stargazin and β-catenin remained robustly associated with GluR2, as expected (Figure 5B) (Dunah et al., 2005). These results suggest that GluR2 and N-cadherin interact closely on the neuronal surface and show that their association requires extracellular disulfide bonding to remain intact in a coimmunoprecipitation assay.

NTD of GluR2 Directly Binds N-Cadherin in Heterologous Cells

To corroborate the interaction between GluR2 and N-cadherin, we tested for their biochemical association when overexpressed in HEK cells. N-cadherin was cotransfected with wild-type GluR2 (Myc-GluR2) or various mutant constructs, or with a GluR2 construct lacking the entire C-terminal tail (GluR2Δ50C), or with NTDR2-pDisplay. As control, we cotransfected N-cadherin with GluR2 lacking the NTD (GluR2ΔNTD) or GluR1 lacking the last

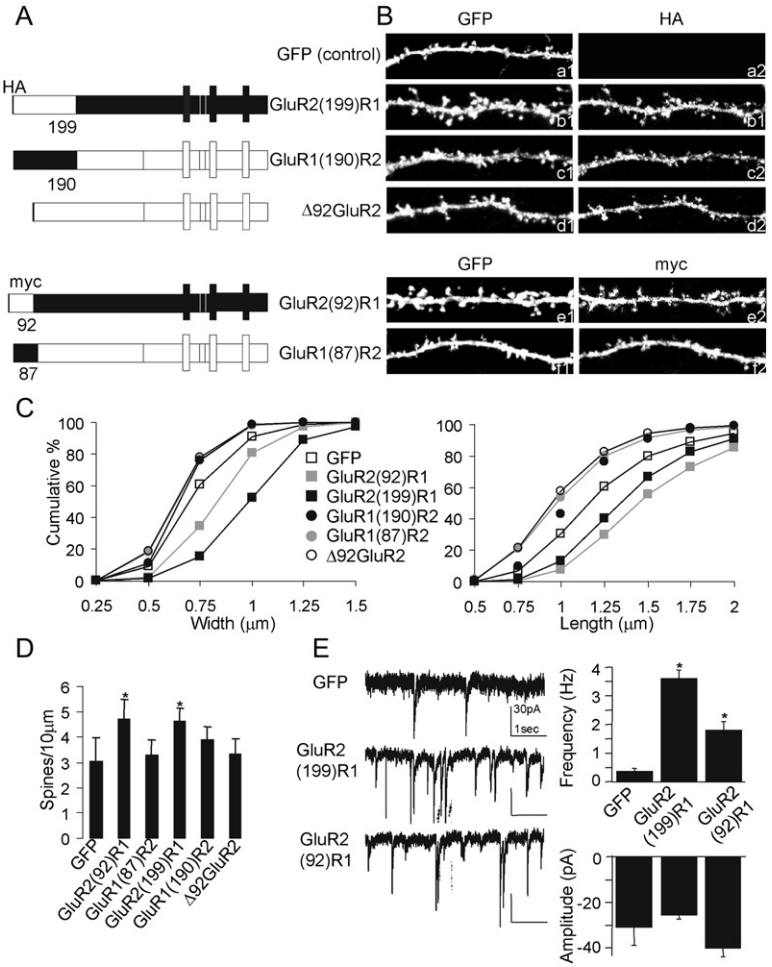

Figure 4. Spine-Inducing Determinants of the Extracellular Domain of GluR2

(A) Diagram of chimeric constructs between GluR1 and GluR2 (all HA or *myc*-tagged at the N terminus).

(B) The hippocampal neurons were transfected with EGFP alone (control) or EGFP plus various HA-GluR constructs, as indicated at left. Each pair of images (a1/a2, b1/b2, etc.) shows the transfected GluR construct stained by HA antibodies (right), and EGFP fluorescence to outline dendrite/spine morphology (left).

(C) Cumulative frequency plots of spine length (μm) and spine head width (μm) in neurons transfected as in (B) (>1000 spines and >18 neurons examined for each construct).

(D) Quantitation of spine density (number of spines per 10 μm dendrite length; mean values ± SEM) in neurons transfected as in (B) (>16 neurons, >180 dendrites examined for each construct). * Histograms show mean values ± SEM *, $p < 0.01$.

(E) Representative traces and average frequency and amplitude histograms (mean ± SEM) of mEPSCs recorded in control neurons (GFP, n = 26) and neurons cotransfected with the indicated plasmids [GluR2(199)1, n = 18; GluR2(99)R1, n = 8] and GFP. Values with an asterisk are significantly different from control ($p < 0.001$).

4 residues (GluR1Δ4C). We used GluR1Δ4C and not GluR1 lacking the entire C-terminal tail, because the latter construct (GluR1ΔC) when overexpressed in HEK cells was poorly expressed on the cell surface and remained mainly intracellular. N-cadherin coimmunoprecipitated with wild-type GluR2, GluR2Δ50C, and GluR2(92)R1, but not with GluR1Δ4C, GluR1(87)R2, GluR2ΔNTD, or Δ92GluR2 (Figure 5C). N-cadherin also coimmunoprecipitated with NTDR2-pDisplay (Figure 5C). These data demonstrate that GluR2 and N-cadherin interact in heterologous cells via the NTD of GluR2, without need for the cytoplasmic tail of GluR2.

Next, we tested whether extracellular soluble immunoglobulin Fc fusion proteins of GluR2-NTD (Fc-NTDR2) or GluR1-NTD (Fc-NTDR1) applied extracellularly could bind specifically to the surface of HEK cells overexpressing N-cadherin. Cell-surface binding of Fc-NTD was detected by anti-Fc antibody conjugated to horseradish peroxidase. Specific binding was calculated by subtracting the binding of Fc-NTD to untransfected HEK cells ("background" binding) from the binding of Fc-NTD to cells transfected with N-cadherin (Figure 5D). Fc-NTDR2 showed robust specific binding to cells expressing N-cadherin; in comparison, Fc-NTDR1 binding to N-cadherin-transfected cells was barely above background (Figure 5D). Furthermore, the first 92 or the first 160 residues of NTDR2 fused to GST, but not GST alone, were able to pull down soluble immunoglobulin Fc fusion proteins of N-cadherin (Figure 5E). Together, these results indicate an extracellular interaction between the NTD of GluR2 and N-cadherin, which is likely to be direct.

We used a cell aggregation assay to test whether N-cadherin and GluR2 expressed on the surface of different cells can interact in *trans*. HEK cells were first separately transfected with N-cadherin-GFP, GluR2-DsRed, NTDR2-DsRed-pDisplay, or DsRed alone. On the following day, the cells were dissociated by trypsin, and an equal number of cells were mixed and incubated under gentle agitation for 90 min in the following combination: N-cadherin-GFP cells plus GluR2-DsRed cells, N-cadherin-GFP plus DsRed, or N-cadherin-GFP plus NTDR2-DsRed-pDisplay. We observed that N-cadherin-expressing cells formed aggregates with themselves (presumably through homophilic interaction) (Figure 6A) but also with cells expressing GluR2-DsRed or NTDR2-DsRed-pDisplay (Figure 6A). To quantify the aggregation, the number of individual

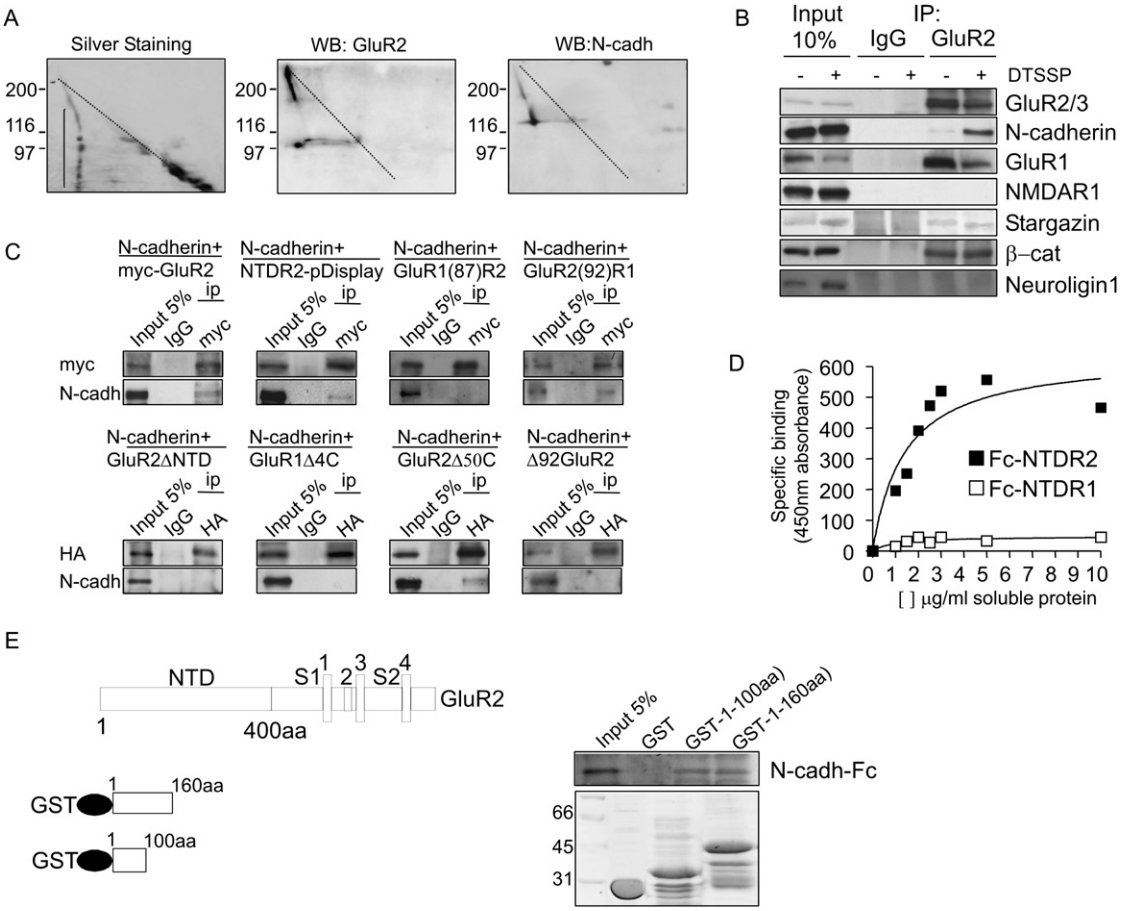

Figure 5. GluR2 and N-Cadherin Are Associated in Neurons, and the NTD of GluR2 Directly Binds N-Cadherin

(A) Silver staining of 2D diagonal gel (see Figure S1 for explanation) of proteins from neurons crosslinked with DTSSP and immunopurified with GluR2 antibodies. The spots and bands below the diagonal indicated the proteins coimmunopurified with GluR2. Immunoblotting shows GluR2 and N-cadherin below the diagonal in the immunopurified preparation.

(B) Hippocampal neuron cultures crosslinked with DTSSP (+) or not crosslinked (–) with DTSSP were immunoprecipitated with GluR2 antibodies and then immunoblotted under reducing conditions to look for coimmunoprecipitation of the indicated proteins.

(C) N-cadherin coimmunoprecipitates with Myc-tagged GluR2, GluR2Δ50C, NTDR2-pDisplay, and GluR2(92)R1, but not with GluR1Δ4C, GluR1(87)R2, GluR2ΔNTD, or Δ92GluR2, from HEK cells cotransfected as indicated.

(D) Direct binding of soluble Fc-NTDR2 or Fc-NTDR1 to HEK cells transfected with N-cadherin.

(E) Western blot analysis of soluble purified Fc-N-cadherin that was pulled down by the first 92 or the first 160 residues of NTDR2 fused to GST is shown. At bottom is shown the Coomassie stain of the GST proteins.

(i.e., not-aggregated) transfected cells in 50 μl was counted immediately after the cells were mixed (N_0) and after 90 min of incubation (N_t). The N_0/N_t ratio is directly related to the number of cells forming aggregates during the 90 min. The N_0/N_t ratio value was high for cells transfected with N-cadherin in all mixture conditions. The N_0/N_t ratio for cells transfected with GluR2-DsRed or NTDR2-DsRed-pDisplay was low when the cells were mixed with untransfected cells, but increased when they were incubated with cells expressing N-cadherin (Figure 6B). Cells transfected with DsRed did not aggregate when mixed with N-cadherin-expressing cells. These findings show that, in heterologous cells, GluR2 (presumably via the NTD) can interact in *trans* with N-cadherin.

N-Cadherin-Coated Beads Recruit GluR2 in Hippocampal Neurons

To investigate the extracellular association of GluR2 and N-cadherin on the surface of neurons, we measured the recruitment of AMPA receptors by N-cadherin-coated beads (Thoumine et al., 2006). Coated beads were applied for 30 min to hippocampal neurons transfected with fluorescently tagged GluR subunits. As positive control, we showed that DsRed-tagged N-cadherin expressed in neurons was recruited to N-cadherin-bearing beads (Figure 7A). The negative controls NR1-Venus and NR2A-Venus showed very slight enrichment under the beads (fluorescence ratio was near 1) (Figures 7B and 7C and Table S2). GluR2 tagged with YFP at its C terminus and

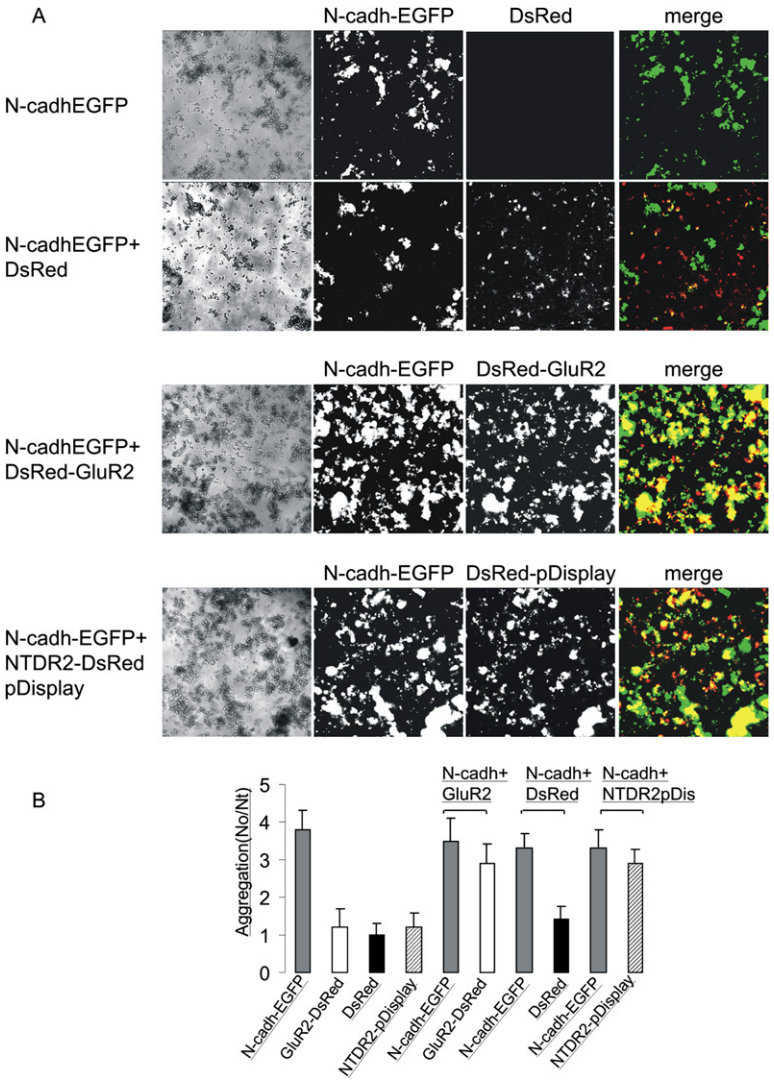

Figure 6. GluR2 NTD and N-Cadherin Can Interact in *trans* in HEK Cells

(A) Equal numbers of HEK cells expressing N-cadherin-EGFP or GluR2-DsRed or DsRed or NTDR2-DsRed-pDisplay were mixed and incubated under gentle agitation for 90 min in the following combinations: N-cadherin-EGFP alone, N-cadherin-EGFP plus DsRed, N-cadherin-EGFP plus GluR2-DsRed cells, or N-cadherin-EGFP plus NTDR2-DsRed-pDisplay, as indicated. N-cadherin-EGFP-expressing cells form aggregates with themselves. GluR2-DsRed cells or NTDR2-DsRed-pDisplay cells form aggregates when mixed with N-cadherin-EGFP-expressing cells.

(B) The histograms show HEK cell aggregation plotted as the number of non-aggregated HEK cells at the time of mixing (N_0) divided by the number of non-aggregate cells after 90 min (N_t). The N_0/N_t ratio is directly related to the number of cells forming aggregates during the 90 min. Histogram shows the mean values ± SEM of seven determinations.

GluR2 tagged with GFP at its N terminus, as well as *myc*-NTDR2-pDisplay (visualized with anti-*myc* staining), accumulated at the N-cadherin-bead contact sites, albeit less strongly than DsRed-N-cadherin. NTDR1-pDisplay and *myc*GluR1(87)R2 were also recruited to N-cadherin beads, but to a lesser extent than NTDR2-pDisplay (Figures 7B and 7C and Table S2). No recruitment of GluR2 was observed by beads coated with the extracellular domain of cadherin 11. In cells cotransfected with N-cadherin-DsRed and GluR2-YFP, there was a strong positive correlation between the amount of recruitment of both proteins under N-cadherin-coated beads (Figure 7D).

We also applied beads coated with an antibody directed against the extracellular region of N-cadherin (Gc4). The Gc4-coated beads recruited GluR2-YFP, GluR2-GFP, and NTDR2-pDisplay (Figures 7B and 7C and Table S2). Again, the recruitment of NR1 and NR2, NTDR1-pDisplay and *myc*GluR1(87)R2 was significantly weaker than that of GluR2 or NTDR2.

The ability of Gc4 beads to recruit GluR2 (presumably secondarily to N-cadherin) suggests that N-cadherin and GluR2 can interact directly or indirectly in *cis* (i.e., in the same postsynaptic membrane). By extrapolation, it is possible that N-cadherin beads also recruit GluR2 secondarily to recruitment of N-cadherin. If that is the case, there should be a direct correlation between the amount of N-cadherin-DsRed accumulated and that of GFP- or YFP-tagged GluR2. We note, however, that relative to N-cadherin-coated beads, Gc4 antibody beads were more effective in recruiting N-cadherin to sites of contact than in recruiting GluR2 (see Figure 7C, green bars). This further suggests that N-cadherin-coated beads can recruit GluR2 by interacting with neuronal surface GluR2 in *trans*.

N-Cadherin Modifies GluR2 Surface Diffusion

To further analyze the functional interaction of N-cadherin and GluR2, we assessed how GluR2 surface diffusion was affected by crosslinking or overexpression of N-cadherin.

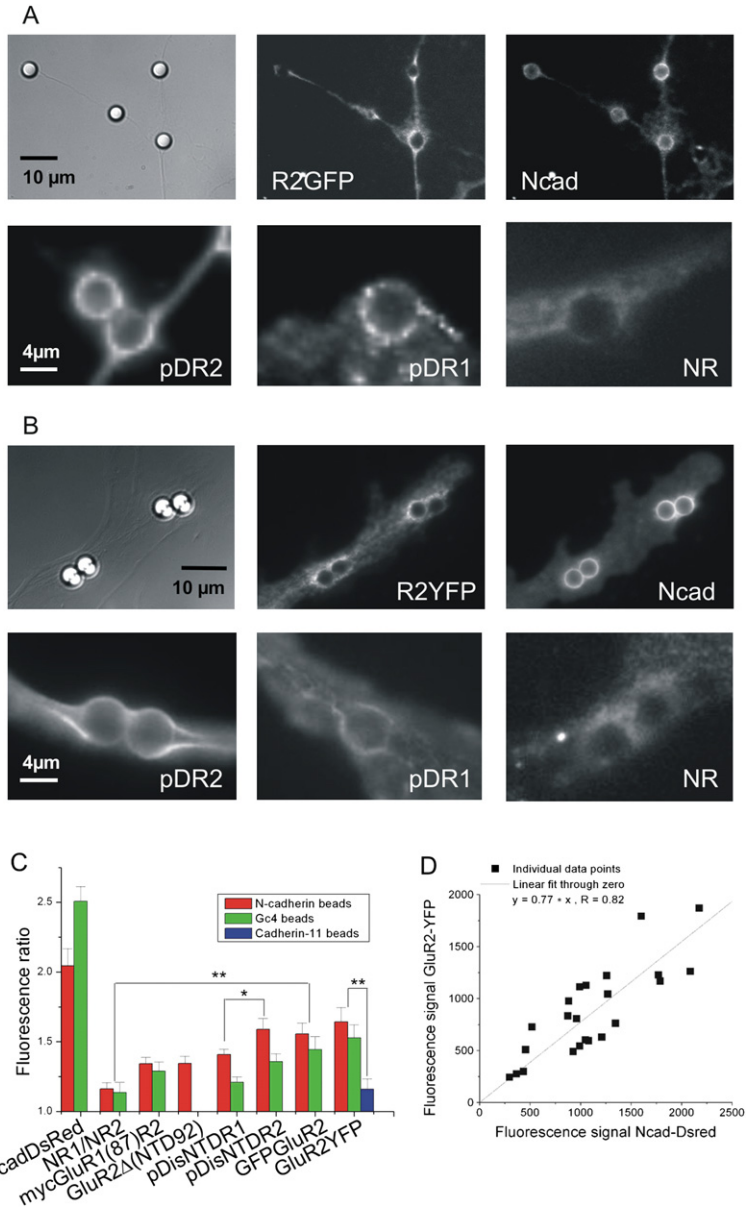

Figure 7. Micrographs Showing the Recruitment of Transfected Receptors by N-Cadherin-Coated Beads

(A) (Top) Images in transmission, GluR2-EGFP fluorescence, and N-cadherin-DsRed fluorescence (N-cadh-DsRed). (Bottom) NTDR2-pDisplay, anti-*myc* staining; NTDR1-pDisplay, anti-*myc* staining; cotransfected NR1-Venus and NR2-Venus.

(B) Micrographs showing the recruitment of transfected receptors by Gc4-coated beads. (Top) Images in transmission, GluR2-YFP fluorescence, and N-cadherin-DsRed fluorescence (N-cadh-DsRed). (Bottom) NTDR2-pDisplay, anti-*myc* staining; NTDR1-pDisplay, anti-*myc* staining; NR: cotransfected NR1-Venus and NR2-Venus.

(C) Fluorescence ratio of cells transfected with each plasmid. Bar graph showing the mean of each distribution ± standard error, plotted for N-cadherin-coated beads and Gc4-coated beads. *$p < 0.05$, **$p < 0.01$. Cadherin-11-coated beads were used as controls on GluR2-YFP-transfected neurons.

(D) Plot of the fluorescence intensity of GluR2-YFP over N-cadherin-DsRed recruited under 23 individual N-cadherin-coated beads. Both proteins displayed a proportional recruitment as shown by the linear fit.

We first monitored the fluorescence recovery after photobleaching (FRAP) of GluR2-GFP enriched at N-cadherin bead contact sites (Figures 8A and 8B). The kinetics of fluorescence recovery was slower at N-cadherin bead regions than in control dendritic regions, suggesting that GluR2 is retained at contact sites through a *trans* interaction with N-cadherin. By analyzing these data using a diffusion trapping model already described for N-cadherin homophilic interactions (Thoumine et al., 2006), we estimated that the lifetime of the N-cadherin-GluR2 *trans* binding is on the order of 25 min, confirming the rather labile interaction demonstrated in biochemical experiments (Figure 8B).

We then performed FRAP experiments on spontaneous GluR2 aggregates on neurons cotransfected with GluR2 and N-cadherin while crosslinking N-cadherins with the Gc4 anti-N-cadherin antibody (Figure 8C). For these experiments we used Super Ecliptic pHluorin (SEP)-GluR2 and N-cadherin-DsRed or L1-GFP and N-cadherin-DsRed. Because of the pH sensitivity of SEP (pHluorin), only GluR2-SEP at the neuronal surface can be detected, whereas GluR2-SEP present in more acidic intracellular compartments is not visible. This allowed us to probe the diffusion of GluR2 at the plasma membrane only. The photobleaching spot was large enough so that both dendritic spines and the dendritic shaft were probed in these measurements. L1-GFP is a transmembrane protein that does not interact with N-cadherin and thus serves as a control to show that the overall membrane environment is not affected by N-cadherin crosslinking. The kinetics of surface GluR2 fluorescence recovery (measured by SEP-GluR2)

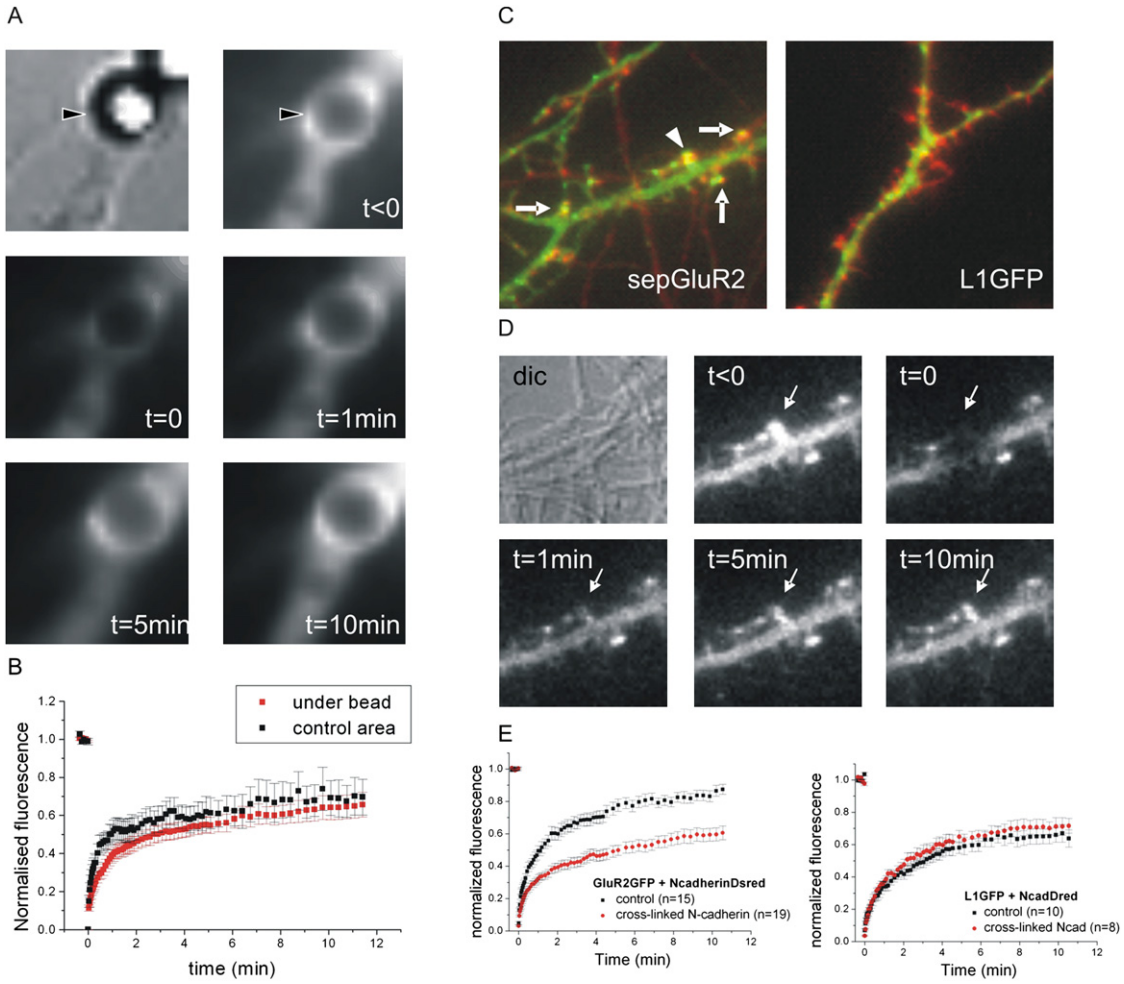

Figure 8. Fluorescence Recovery after Photobleaching of GluR2 under N-Cadherin-Coated Beads and with N-Cadherin Cross-linking

(A) Micrographs illustrating the photobleaching experiment on GluR2-YFP fluorescence enriched at contact site of N-cadherin-coated bead. On the transmission image, a bead that triggers a recruitment of GluR2-YFP is shown (head). Images before the laser bleaching, just after the bleaching, and at 1, 5, and 10 min after the bleaching are shown. Images are 10 μm × 10 μm.

(B) Plot of the recovery of fluorescence after photobleaching on N-cadherin-coated bead contact sites (n = 20) compared to control areas (n = 7) normalized to the prebleach fluorescence. Data are expressed as mean ± SEM. The kinetics of the fluorescence recovery is different for the two curves.

(C) Micrographs showing the merged fluorescence signals of Super Ecliptic pHluorin (SEP)-GluR2 and N-cadherin-Dsred (left) or L1-GFP and N-cadherin-Dsred (right) (image size is 25 μm × 25 μm). Sites of colocalization of sepGluR2 and N-cadherin are shown by arrows. The arrowhead shows the region that is photobleached.

(D) Micrographs (12.5 μm × 12.5 μm) illustrating the photobleaching experiment on a SEP-GluR2 fluorescence aggregate. Images before the laser pulse, just after the bleaching, and at 1, 5, and 10 min after the bleaching are shown.

(E) The fluorescence recovery in the presence or absence of anti-N-cadherin preaggregated antibodies was monitored. We could see no difference between the fluorescence recovery of L1-GFP with or without Gc4 incubation, whereas SEP-GluR2 fluorescence recovery is markedly delayed when incubated with Gc4 immobilizing antibody.

was markedly slowed when N-cadherins were crosslinked (Figures 8C–8E). The effect of N-cadherin crosslinking was specific for GluR2 as it did not affect the mobility of L1-GFP. These data suggest a *cis* interaction between N-cadherin and GluR2 with substantial longer lifetime than the *trans* interaction.

Together, these experiments indicate that immobilizing N-cadherins with either beads or crosslinking antibodies reduces GluR2 surface diffusion, thus providing further evidence for a functional interaction between GluR2 and N-cadherin on the neuronal surface.

Inhibition of Synapse Morphology and Function by Knockdown of N-Cadherin

Finally, we inhibited expression of N-cadherin proteins in hippocampal neurons by plasmid-based expression of

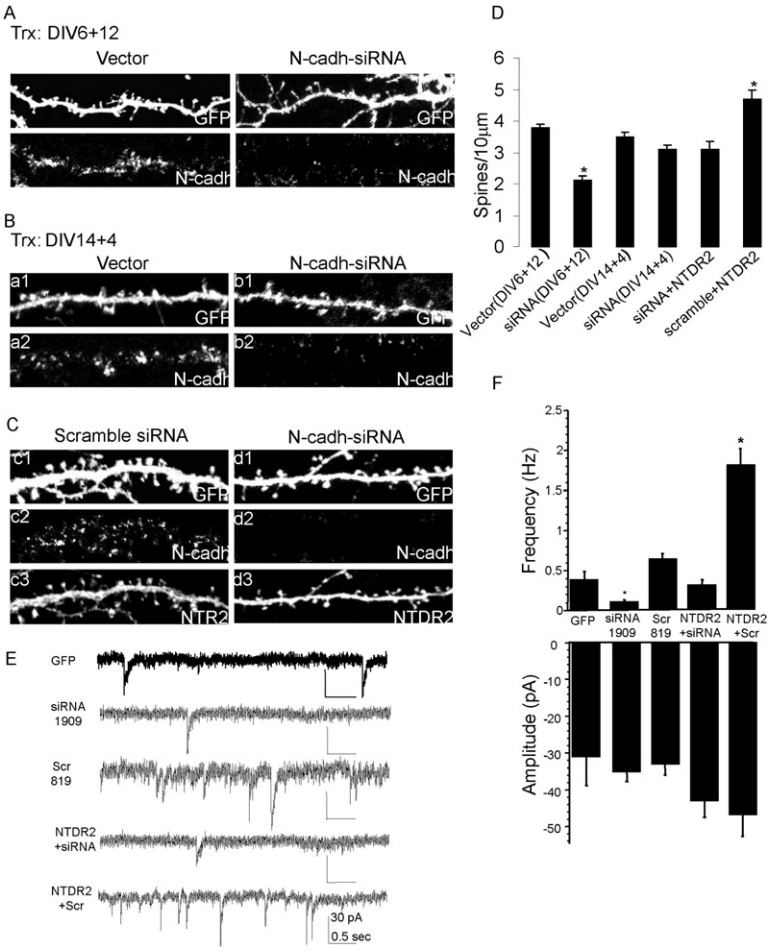

Figure 9. siRNA Knockdown of N-Cadherin Prevents the Effect of GluR2NTD on Spine Morphology and Synaptic Function

(A) Cultured hippocampal neurons transfected (Trx) on DIV6 with Pll3.7-EGFP vector or N-cadh-siRNA and labeled on DIV18 for N-cadherin and EGFP, as indicated in each pair of images.

(B) Hippocampal neurons were transfected on DIV14 with Pll3.7-EGFP or N-cadh-siRNA and labeled on DIV18 for N-cadherin and EGFP, as indicated in each pair of panels.

(C) Hippocampal neurons were transfected (Trx) on DIV14 with N-cadh-siRNA plus NTDR2-pDisplay or siRNA scramble plus NTDR2-pDisplay and labeled on DIV18.

(D) Quantification of spine density on hippocampal neurons transfected on DIV6 and labeled at DIV18 and neurons transfected on DIV14 and labeled on DIV18 (number of spines per 10 μm; 12 neurons for each treatment). *$p < 0.01$.

(E and F) Samples traces (E) and average frequency and amplitude histograms (mean ± SEM; [F]) of mEPSCs recorded from control neurons (GFP, n = 26) and neurons cotransfected with the indicated plasmids (siRNA1909, n = 10; scramble819, n = 8; NTDR2 + siRNA1909, n = 10; NTDR2 + scramble819, n = 8) and GFP. In (F), values with an asterisk are significantly different from control ($p < 0.001$).

small interfering RNA (siRNA; N-cadherin immunostaining intensity was decreased to <10% of vector-transfected controls). DIV6 neurons transfected with N-cadherin siRNA (siRNA1909) for 12 days (DIV6 + 12) showed a reduced number of spines (Figures 9A and 9D). Neurons transfected with N-cadherin-siRNA at DIV14 for 4 days showed no significant change in spine morphology or density (Figures 9B and 9C and Table 1). It is important to note, however, cotransfection of N-cadherin-siRNA (DIV14 + 4), but not of scrambled N-cadherin-siRNA (siRNA 819), prevented the promoting effect of NTDR2-pDisplay or of GluR2(199)R1 on spine morphology and number (Figures 9B and 9C and Table 1). Neurons cotransfected with NTDR2-pDisplay or GluR2(199)R1 and a scrambled N-cadherin-siRNA sequence showed increased length, width, and density of spines (Figures 9C and 9D and Table 1).

We also tested the effects of N-cadherin-siRNA (siRNA 1909) or scrambled N-cadherin-siRNA (Scr 819), alone or in combination with the NTDR2-pDisplay (NTDR2), on mEPSCs (Figures 9E and 9F). N-cadherin-siRNA, but not scrambled N-cadherin-siRNA, by itself decreased the frequency of mEPSCS. This suggests that the N-cadherin siRNA decreased the number of excitatory release sites, as expected from knockdown of endogenous N-cadherin expression. Coexpression with N-cadherin-siRNA completely inhibited the facilitatory effect of NTDR2-pDisplay on mEPSCs (compare NTDR2 + siRNA in Figures 9E and 9F to NTDR2 in Figure 3B). Indeed, coexpression of NTDR2-pDisplay with N-cadherin-siRNA restored the frequency of mEPSC to the control level (Figure 9F). This effect was probably due to a residual expression of N-cadherin, resulting from incomplete knockdown by N-cadherin-siRNA. The scrambled N-cadherin-siRNA (Scr 819) had no effect on mEPSCs, and it did not prevent the increase in mEPSC frequency induced by NTDR2-pDisplay (Figure 9F). These data indicate that normal expression of N-cadherin is essential for GluR2 NTD to exert its effect on spine morphogenesis and on synaptic function.

DISCUSSION

In this study we demonstrate a specific biochemical function and cell-biological activity of the NTD of GluR2. The NTD is sufficient to promote spine morphogenesis when

placed extracellularly on a heterologous membrane protein. In spines enlarged by NTDR2 there was increased accumulation of synaptophysin, bassoon, shank, and N-cadherin. Together with the enhanced minis and FM1-43 staining, these data suggest that NTDR2 induces an increase in the number, size, and function of synapses.

We observed an increase in the frequency, but not amplitude, of mEPSCs following expression of the NTDR2 in cultured hippocampal neurons. A similar change in frequency has been previously described in neurons transfected with postsynaptic proteins PSD-95 (El-Husseini et al., 2000), shank1 (Sala et al., 2001), and shank3 (Roussignol et al., 2005). This effect was tentatively attributed by these and other authors to an unidentified retrograde signal. However, more recently, an effect on frequency rather than amplitude of mEPSCs has been observed upon knockdown of PSD-95 (Elias et al., 2006), which is well established as a postsynaptic scaffold protein that recruits AMPA receptors and enhances AMPA receptor-mediated EPSCs. We believe that GluR2-NTD provides another example of a postsynaptic manipulation that alters AMPA-mediated synaptic transmission and that has a selective effect on mini frequency, perhaps as a consequence of an increased number of functional synapses. If a retrograde signal is to be invoked, our study suggests N-cadherin as a good candidate, a homophilic adhesion molecule that we found binds directly to the NTD of GluR2.

Previous studies have suggested a connection between AMPA receptors and N-cadherin (Dunah et al., 2005; Jones et al., 2002; Nuriya and Huganir, 2006). In particular, Nuriya et al. and Dunah et al. demonstrated, in brain and in heterologous cells, a biochemical association of N-cadherin and AMPA receptors by coimmunoprecipitation. The important advance in our study is the demonstration of a direct interaction between GluR2 and N-cadherin that occurs extracellularly via the NTD domain. Our results are at odds with Nuriya et al. (Nuriya and Huganir, 2006), who reported that N-cadherin can be coimmunoprecipitated with all AMPA receptor subunits in heterologous cells. We believe the discrepancies can be explained if the association of GluRs and N-cadherin shown in Nuriya's work is indirect, perhaps mediated by other proteins and resulting from more gentle solubilization detergents (Nuriya and Huganir, 2006).

Using an unbiased approach (surface crosslinking followed by immunoprecipitation and mass spectrometric identification of GluR2-interacting proteins), we showed that N-cadherin is a major extracellular binding partner of GluR2 in neurons. Given that N-cadherin is a well-established player in synapse development and spine morphogenesis (Benson and Tanaka, 1998; Fannon and Colman, 1996; Takeichi and Abe, 2005; Tanaka et al., 2000; Togashi et al., 2002), our findings likely explain why overexpression of GluR2 induces bigger and more abundant spines depending on its NTD, why knockdown of GluR2 impairs spine morphogenesis, and why the soluble Fc-NTDR2, but not Fc-NTDR1, reduced spine density when added to culture medium (Passafaro et al., 2003). Further clarification of the functional significance of GluR2-N-cadherin interaction, however, will require additional confirmation in vivo. Ideally, this would entail generation of a knockin mutation of the GluR2-NTD that prevents its interaction with cadherin, while preserving subunit assembly of AMPA receptors.

We propose that GluR2 and N-cadherin interact via extracellular domains at excitatory synapses and that this NTD-dependent complex promotes the growth and maintenance of spines. The interaction appears less stable than that of GluR2 with GluR1 or stargazin, insofar as it requires extracellular crosslinking to maintain integrity during coimmunoprecipitation in neurons. Thus the association between NTD and N-cadherin might occur at low affinity or transiently, which is perhaps not surprising, given their extracellular nature. N-cadherin is also associated with LAR receptor tyrosine phosphatase and cytoplasmic catenins, and LAR can promote the synaptic recruitment of AMPA receptors, N-cadherin, and β-catenin, all of which would promote the growth of dendritic spines (Dunah et al., 2005). Moreover cadherins can also modulate the activity and localization of signal molecules such as cortactin, Arp2/3, formin-1, and the Rho family of GTPases, which also impact spine formation and stability (Takeichi and Abe, 2005).

The synaptic trafficking of AMPA receptors, including GluR2, is highly regulated and important for determining synaptic strength (Malinow and Malenka, 2002). We propose that accumulation of GluR2-containing AMPA receptors at the synapse promotes recruitment of N-cadherin and associated molecules, thereby stabilizing and enlarging the synapse. In this way, GluR2 can be considered as having a "structural" role. GluR2 and N-cadherin, by virtue of their reciprocal interaction, could mutually support each other's accumulation at synaptic sites. This process could be analogous to how shank and homer, two PSD scaffold proteins, cooperate to induce the maturation and enlargement of dendritic spines in primary cultures of hippocampal neurons (Sala et al., 2001).

N-cadherin is present on both sides of the synapse, whereas AMPA receptors are primarily postsynaptic in location. Whether GluR2 binds to N-cadherin primarily in *cis* or in *trans* remains open, but our cell aggregation experiments, Fc-fusion protein binding assays, and bead aggregation data all indicate that the GluR2-N-cadherin interaction can occur in *trans* as well as in *cis*. In any case, since N-cadherin itself binds homophilically across the synaptic cleft, GluR2 can presumably associate with a *trans*-synaptic cadherin protein complex. In this way, a subunit of a glutamate receptor channel whose abundance correlates with synaptic strength can interact with an adhesion complex involved in regulation of synapse morphology. Thus, the GluR2-N-cadherin interaction provides an attractive mechanism that would contribute to the coordinate regulation of synapse function and morphology.

The size of the AMPA receptor complex measured by EM suggests that it can extend ~20 nm extracellularly from the postsynaptic membrane (Nakagawa et al., 2005),

leaving the NTD well positioned to bind to proteins in or spanning the synaptic cleft. How might GluR2-NTD and N-cadherin interact in terms of three-dimensional structure? We modeled the cadherin-binding surface of GluR2-NTD, and the mode of interaction between the cadherin extracellular domain and GluR2-NTD, based on the known 3D structures of cadherin and of proteins homologous to GluR2-NTD. In our GluR-2NTD model (obtained by homology modeling with the mGluR1 extracellular ligand-binding region and generated with the use of Modeler and evaluated by Verify3D), the first 92 amino acids of the NTD that bind to N-cadherin are on the surface of the NTD and therefore accessible for protein interactions (Figure S3). We also used the protein-docking algorithm Bimolecular complex Generation with Global Evaluation and Ranking (BiGGER) integrated in the molecular modeling software Chemera 3.0 (Palma et al., 2000) to predict the mode of extracellular binding between N-cadherin (using the crystallographic structure of C-cadherin ectodomain [Boggon et al., 2002]) and GluR2 (using GluR2-NTD structure obtained by homology modeling). The predicted interaction sites lay on the internal side of EC3 and EC2 of the five tandem cadherin ectodomains (EC1-EC5) (Figure S4). In addition, the predicted interaction sites were separate from the cadherin-cadherin *trans* and *cis* interaction interfaces (which are mediated by EC1) (Boggon et al., 2002). Thus, the modeled site of interaction with GluR2-NTD occurs at an "available" place on the extracellular region of cadherin that does not have any known protein interactions.

In conclusion, we provide evidence of a direct interaction between a subunit of the ionotropic glutamate receptor AMPA and a synaptic adhesion molecule. These findings have interesting implications for coordinate regulation of structure and function of synapses.

EXPERIMENTAL PROCEDURES

DNA Constructs

HA and Myc epitope tags were inserted three amino acids C-terminal of the signal peptide of GluR subunits. NTDR2-pDisplay and NTDR1-pDisplay chimeras were made by fusing amino acids 1–400 of GluR2 or GluR1 to the pDisplay vector or the transmembrane domain of CD4. The deletion constructs were made by PCR amplification with appropriate oligos. The plasmids used in the bead-binding experiments were pcDNA *myc* GluR2-YFP (tagged at −22, near the C terminus), pcDNA *myc* GluR2-EGFP (N-terminal tag), NTDR1, NTDR2, cotransfected pRcCMVaa NR1-Venus and NR2A-Venus (N-terminal tag) (a gift from Jacques Neyton, Ecole Normale Supérieure, Paris), pEGFP N1 N-cadherin-EGFP (C-terminal tag), and pcDNA3 N-cadherin-dDsred (a gift from Mireille Lambert, INSERM U440-UPMC, Paris). The hFc-N-cadherin chimera was used on the beads, as previously described (Lambert et al., 2000).

For plasmid-based RNA inhibition of N-cadherin, the oligonucleotides annealed and inserted into HpaI/Xho1 of the PII 3.7 vector (Rubinson et al., 2003) were 5′-atcgatatatgcaacagaa-3′ for N-cadherin-siRNA and 5′-gccgatgaaggaaccacatga-3′ for scramble siRNA. The specificity and efficacy of this construct in interfering with N-cadherin expression was first tested in heterologously expressed N-cadherin in HEK cells.

Cell Cultures and Transfection

Primary hippocampal neurons were prepared from embryonic days 18–19 rat brains (Brewer et al., 1993) and placed on coverslips coated with poly-D-lysine (30 μg/ml) and laminin (2 μg/ml) at a density of 75,000/well for immunochemistry, and at 300,000/well for biochemistry experiments. After 13–14 days in vitro, the cultures were transfected using the calcium phosphate method. For the bead-binding experiments, the neurons were transfected with Effectene transfection reagent (QIAGEN) after 4 days in vitro.

Immunostaining and Antibodies

The transfected neurons were fixed for 8 min in 4% paraformaldehyde plus 4% sucrose and immunostained as described (Passafaro et al., 2003). The antibodies/probes were rabbit anti-HA (Santa Cruz Biotechnology, Santa Cruz, CA; 1 μg/ml), -GluR2/3 (Chemicon, International S.C.), -GluR1C-term (Chemicon International), -N-Cadherin (BD Biosciences PharMingen), -NLG1 (SYSY, Gottingen, Germany), β-catenin (gift from Grazia Pietrini, IN-CNR, Milan), and monoclonal: anti NMDAR1 (BD Biosciences PharMingen) and anti -GAD (GAD -6; Developmental Studies Hybridoma Bank, University of Iowa, IA); anti-GST monoclonal (Santa Cruz Biotechnology, Santa Cruz, CA); Alexa 568 and Alexa 488 secondary antibodies (Molecular Probes, Eugene, Oregon).

In Vivo Crosslinking of Hippocampal Neurons and Coimmunoprecipitation Studies

Hippocampal neurons plated on coverslips coated with poly-D-lysine (30 μg/ml) and laminin (2 μg/ml) at a density of 300,000/well were washed once with D-PBS and crosslinked with 2 mM dithiobis (sulfosuccinimidylpropionate) (DTSSP) (Pierce Chemical Co., Rockford, IL) in D-PBS. After 30 min incubation at room temperature, the reaction was quenched in 50 mM Tris-HCl, pH 7.4, for 15 min. The crosslinked neurons were then washed with D-PBS and incubated for 1 hr at 4°C with a buffer containing 50 mM Tris-HCl, 150 mM NaCl, 1 mM EDTA, 1% Triton X-100, 1% saponin (BST Buffer), complete EDTA (Roche). Two-dimensional diagonal gel electrophoresis was performed as described (Chan et al., 1998). Coimmunoprecipitation experiments from neurons were performed as described (Dunah et al., 2005). The HEK immunoprecipitation experiments were performed as previously described (Hsueh and Sheng, 1999).

In Vitro Binding Assay and GST Pull-Down

HEK cells transfected or not with N-cadherin were incubated for 2 hr with different concentrations of Fc-NTDR2 or Fc-NTDR1 at RT and then washed, fixed, and incubated for 30 min with Fc antibody conjugated to horseradish peroxidase. The Fc-NTD fusion proteins were prepared as previously described (Passafaro et al., 2003). For pull-down assay, the extracellular regions of GluR2 (aa 1–100) and (aa 1–160) were subcloned into pGEX vector (Clontech).

Fc-N-Cadh-Coated Bead Preparation, Incubation, and Immunocytochemistry

Ten microliter of 4 μm latex microspheres (sulfated, 8% solids, Ideal Latex Corp) were incubated overnight at room temperature with 10 μg goat anti-human Fc antibodies (Jackson Immunoresearch), rinsed in borate buffer (0.2 M, pH 8.5) containing 0.3% globulin-free BSA (Sigma), then incubated with 2 μg chimera hFc-N-cadherin for 3 hr at room temperature, rinsed again, and used within 1 day if kept on ice. We also used beads coated with anti-N-cadherin antibodies (clone Gc4, Sigma), coupled via goat anti-mouse Fc antibodies (Jackson Immunoresearch).

Beads coated with anti-N-cadherin antibodies (clone Gc4, Sigma), coupled via goat anti-mouse Fc antibodies (Jackson Immunoresearch), were mixed with medium + 1% BSA (to avoid unspecific binding) and incubated on neurons for 30–60 min at 37°C (2.7E6 beads in 1 ml). The beads were mixed with medium + 1% BSA (to avoid nonspecific binding) and incubated on neurons for 30 min to 1 hr at 37°C

(beads in 1 ml). We then rinsed the cells three times with warm medium and fixed with PFA 4% sucrose.

Bead Recruitment Analysis

To quantify the recruitment of receptors under the beads, average fluorescence intensity was measured in a ring under the bead (F bead) and on control neurites or lamellipodia (Fctl), both corrected for the background, and the results were used to compute a fluorescence ratio R = Fbead/Fctl. The data obtained from the indicated number (n) of beads were expressed as mean ± SEM and compared by Student's t test.

Fluorescence Recovery after Photobleaching

The set-up and methods to analyze fluorescence recovery were described previously (Thoumine et al., 2006). Briefly, a single spot Argon laser beam coupled to a fluorescence microscope is used to photobleach selected areas of neurons expressing GFP-tagged receptors and monitor fluorescence recovery. FRAP experiments were performed on GluR2-GFP accumulated at N-cadherin bead contacts, or on GluR2-SEP clusters induced by antibody ligation of cotransfected N-cadherin. Hippocampal rat neurons were transfected at DIV7 and processed 1 week later. Gc4 anti-N-cadherin (1:50) preclustered with a goat anti-mouse Ig secondary antibody (1:100) (Molecular Probes) was added to neurons for 10 min prior to the experiment, in order to immobilize transfected N-cadherin. SEP-GluR2 was a gift from J. Henley (Bristol, UK). L1-GFP was a gift from T. Galli (Paris, France).

Cell Aggregation Assay

HEK cells transfected with the different constructs were trypsinized, counted, and mixed, and the cell mixtures were incubated at 37°C for 90 min under gentle agitation and then plated. The extent of cell/cell aggregation was measured as described (Nguyen and Sudhof, 1997). Random fields were chosen using at 10× objective.

FM1-43 Staining

FM1-43 staining was performed by incubating neurons for 1 min in 6 μm FM1-43 (Molecular Probes) in high potassium buffer followed by two washes in Tyrode solution in the presence of 1 μM tetrodotoxin (TTX) as described (Hering et al., 2003).

Image Analysis

Labeled transfected neurons were chosen randomly for quantification from six coverslips from six independent experiments for each construct. Fluorescence images and morphometric measurements were made as described (Passafaro et al., 2003).

Electrophysiology

The neurons were continuously perfused with the following external medium (mM): NaCl (140), $CaCl_2$ (2), KCl (3), HEPES (10), D-glucose (10), tetrodotoxin (0.0003), bicuculline (0.01), pH 7.4 and osmolarity 330 mOsm. Neurons cotransfected with GFP and NTDR1 or NTDR2 were selected on the basis of their fluorescence and recorded at RT using the whole-cell configuration of the patch-clamp technique. The recording pipettes had a resistance of 3–5 MOhms when filled with the following medium (mM) KCl (140), HEPES (10), D-glucose (10), pH 7.2 and osmolarity 300 mOsm. Miniature EPSCs (mEPCs) were recorded at −65 mV membrane potential through an Axopatch 200B amplifier (Axon Instruments; Union City, CA), filtered at 1 kHz and then digitized at 3 kHz using Axotape (Axon Instruments). Currents were analyzed using the pClamp 9 software (Axon Instruments). All the detected events were re-examined and accepted or rejected on the basis of visual examination. Once more than 100 events had been collected from a neuron, the average frequency and amplitude of these events were measured on the total duration of the sample. Data obtained from the indicated number (n) of cells were expressed as the mean ± SEM and analyzed using the Student's t test.

Supplemental Data

The Supplemental Data for this article can be found online at http://www.neuron.org/cgi/content/full/54/3/461/DC1/.

ACKNOWLEDGMENTS

Thanks to Valentina Bonetti for mass spectrometry analysis, Teru Nakagawa for pDisplay constructs, Mireille Lambert for the production of the hFc-N-cadherin chimera, and Romana Tomasoni for technical assistance and comments. The work was supported by Telethon-Italy (M.P.), the Giovanni Armenise-Harvard Foundation Career Development Program (C.S.), AIRC, European Community (LSHM-CT-2004-511995, SYNSCAFF). M.S. is an Investigator of Howard Hughes Medical Institute. The authors declare that they have no competing financial interests.

Received: June 1, 2006
Revised: February 13, 2007
Accepted: April 16, 2007
Published: May 2, 2007

REFERENCES

Armstrong, N., Sun, Y., Chen, G.-Q., and Gouaux, E. (1998). Structure of a glutamate-receptor ligand-binding core in complex with kainate. Nature *395*, 913–917.

Ayalon, G., and Stern-Bach, Y. (2001). Functional assembly of AMPA and kainate receptors is mediated by several discrete protein-protein interactions. Neuron *31*, 103–113.

Bamji, S.X. (2005). Cadherins: actin with the cytoskeleton to form synapses. Neuron *47*, 175–178.

Beesley, P.W., Mummery, R., and Tibaldi, J. (1995). N-cadherin is a major glycoprotein component of isolated rat forebrain postsynaptic densities. J. Neurochem. *64*, 2288–2294.

Benson, D.L., and Tanaka, H. (1998). N-cadherin redistribution during synaptogenesis in hippocampal neurons. J. Neurosci. *18*, 6892–6904.

Boggon, T.J., Murray, J., Chappuis-Flament, S., Wong, E., Gumbiner, B.M., and Shapiro, L. (2002). C-cadherin ectodomain structure and implications for cell adhesion mechanisms. Science *296*, 1308–1313.

Bozdagi, O., Shan, W., Tanaka, H., Benson, D.L., and Huntley, G.W. (2000). Increasing numbers of synaptic puncta during late-phase LTP: N-cadherin is synthesized, recruited to synaptic sites, and required for potentiation. Neuron *28*, 245–259.

Brewer, G.J., Torricelli, J.R., Evege, E.K., and Price, P.J. (1993). Optimized survival of hippocampal neurons in B27-supplemented Neurobasal, a new serum-free medium combination. J. Neurosci. Res. *35*, 567–576.

Chan, Y.M., Bonnemann, C.G., Lidov, H.G., and Kunkel, L.M. (1998). Molecular organization of sarcoglycan complex in mouse myotubes in culture. J. Cell Biol. *143*, 2033–2044.

Chappuis-Flament, S., Wong, E., Hicks, L.D., Kay, C.M., and Gumbiner, B.M. (2001). Multiple cadherin extracellular repeats mediate homophilic binding and adhesion. J. Cell Biol. *154*, 231–243.

Dingledine, R., Borges, K., Bowie, D., and Traynelis, S.F. (1999). The glutamate receptor ion channels. Pharmacol. Rev. *51*, 7–61.

Dunah, A.W., Hueske, E., Wyszynski, M., Hoogenraad, C.C., Jaworski, J., Pak, D.T., Simonetta, A., Liu, G., and Sheng, M. (2005). LAR receptor protein tyrosine phosphatases in the development and maintenance of excitatory synapses. Nat. Neurosci. *8*, 458–467.

El-Husseini, A.E., Schnell, E., Chetkovich, D.M., Nicoll, R.A., and Bredt, D.S. (2000). PSD-95 involvement in maturation of excitatory synapses. Science *290*, 1364–1368.

Elias, G.M., Funke, L., Stein, V., Grant, S.G., Bredt, D.S., and Nicoll, R.A. (2006). Synapse-specific and developmentally regulated

targeting of AMPA receptors by a family of MAGUK scaffolding proteins. Neuron *52*, 307–320.

Elste, A.M., and Benson, D.L. (2006). Structural basis for developmentally regulated changes in cadherin function at synapses. J. Comp. Neurol. *495*, 324–335.

Fannon, A.M., and Colman, D.R. (1996). A model for central synaptic junctional complex formation based on the differential adhesive specificities of the cadherins. Neuron *17*, 423–434.

Fiala, J.C., Allwardt, B., and Harris, K.M. (2002). Dendritic spines do not split during hippocampal LTP or maturation. Nat. Neurosci. *5*, 297–298.

Gumbiner, B.M. (2005). Regulation of cadherin-mediated adhesion in morphogenesis. Nat. Rev. Mol. Cell Biol. *6*, 622–634.

Harris, K. (1999). Structure, development, and plasticity of dendritic spines. Curr. Opin. Neurobiol. *9*, 343–348.

Harris, K., and Kater, S. (1994). Dendritic spines: cellular specializations imparting both stability and flexibility to synaptic function. Annu. Rev. Neurosci. *17*, 341–371.

Hering, H., and Sheng, M. (2001). Dendritic spines: structure, dynamics and regulation. Nat. Rev. Neurosci. *2*, 880–888.

Hering, H., Lin, C.C., and Sheng, M. (2003). Lipid rafts in the maintenance of synapses, dendritic spines, and surface AMPA receptor stability. J. Neurosci. *23*, 3262–3271.

Hsueh, Y.-P., and Sheng, M. (1999). Requirement of N-terminal cysteines of PSD-95 for PSD-95 multimerization and ternary complex formation, but not for binding to potassium channel Kv1.4. J. Biol. Chem. *174*, 532–536.

Jones, S.B., Lanford, G.W., Chen, Y.H., Moribito, M., Kim, K., and Lu, Q. (2002). Glutamate-induced delta-catenin redistribution and dissociation from postsynaptic receptor complexes. Neuroscience *115*, 1009–1021.

Kopec, C.D., Li, B., Wei, W., Boehm, J., and Malinow, R. (2006). Glutamate receptor exocytosis and spine enlargement during chemically induced long-term potentiation. J. Neurosci. *26*, 2000–2009.

Lambert, M., Padilla, F., and Mege, R.M. (2000). Immobilized dimers of N-cadherin-Fc chimera mimic cadherin-mediated cell contact formation: contribution of both outside-in and inside-out signals. J. Cell Sci. *113*, 2207–2219.

Maddon, P.J., Littman, D.R., Godfrey, M., Maddon, D.E., Chess, L., and Axel, R. (1985). The isolation and nucleotide sequence of a cDNA encoding the T cell surface protein T4: a new member of the immunoglobulin gene family. Cell *42*, 93–104.

Malinow, R., and Malenka, R.C. (2002). AMPA receptor trafficking and synaptic plasticity. Annu. Rev. Neurosci. *25*, 103–126.

Masuko, T., Kashiwagi, K., Kuno, T., Nguyen, N.D., Pahk, A.J., Fukuchi, J., Igarashi, K., and Williams, K. (1999). A regulatory domain (R1-R2) in the amino terminus of the N-methyl-D- aspartate receptor: effects of spermine, protons, and ifenprodil, and structural similarity to bacterial leucine/isoleucine/valine binding protein. Mol. Pharmacol. *55*, 957–969.

Murase, S., Mosser, E., and Schuman, E.M. (2002). Depolarization drives beta-catenin into neuronal spines promoting changes in synaptic structure and function. Neuron *35*, 91–105.

Nakagawa, T., Cheng, Y., Ramm, E., Sheng, M., and Walz, T. (2005). Structure and different conformational states of native AMPA receptor complexes. Nature *433*, 545–549.

Nakai, Y., and Kamiguchi, H. (2002). Migration of nerve growth cones requires detergent-resistant membranes in a spatially defined and substrate-dependent manner. J. Cell Biol. *159*, 1097–1108.

Nguyen, T., and Sudhof, T.C. (1997). Binding properties of neuroligin 1 and neurexin 1beta reveal function as heterophilic cell adhesion molecules. J. Biol. Chem. *272*, 26032–26039.

Nimchinsky, E.A., Sabatini, B.L., and Svoboda, K. (2002). Structure and function of dendritic spines. Annu. Rev. Physiol. *64*, 313–353.

Nose, A., Tsuji, K., and Takeichi, M. (1990). Localization of specificity determining sites in cadherin cell adhesion molecules. Cell *61*, 147–155.

Nuriya, M., and Huganir, R.L. (2006). Regulation of AMPA receptor trafficking by N-cadherin. J. Neurochem. *97*, 652–661.

O'Hara, P.J., Sheppard, P.O., Thogersen, H., Venezia, D., Haldeman, B.A., McGrane, V., Houamed, K.M., Thomsen, C., Gilbert, T.L., and Mulvihill, E.R. (1993). The ligand-binding domain in metabotropic glutamate receptors is related to bacterial periplasmic binding proteins. Neuron *11*, 41–52.

Okamura, K., Tanaka, H., Yagita, Y., Saeki, Y., Taguchi, A., Hiraoka, Y., Zeng, L.H., Colman, D.R., and Miki, N. (2004). Cadherin activity is required for activity-induced spine remodeling. J. Cell Biol. *167*, 961–972.

Palma, P.N., Krippahl, L., Wampler, J.E., and Moura, J.J. (2000). BiGGER: a new (soft) docking algorithm for predicting protein interactions. Proteins *39*, 372–384.

Paoletti, P., Perin-Dureau, F., Fayyazuddin, A., Le Goff, A., Callebaut, I., and Neyton, J. (2000). Molecular organization of a zinc binding n-terminal modulatory domain in a NMDA receptor subunit. Neuron *28*, 911–925.

Passafaro, M., Nakagawa, T., Sala, C., and Sheng, M. (2003). Induction of dendritic spines by an extracellular domain of AMPA receptor subunit GluR2. Nature *424*, 677–681.

Pertz, O., Bozic, D., Koch, A.W., Fauser, C., Brancaccio, A., and Engel, J. (1999). A new crystal structure, Ca2+ dependence and mutational analysis reveal molecular details of E-cadherin homoassociation. EMBO J. *18*, 1738–1747.

Roussignol, G., Ango, F., Romorini, S., Tu, J.C., Sala, C., Worley, P.F., Bockaert, J., and Fagni, L. (2005). Shank expression is sufficient to induce functional dendritic spine synapses in aspiny neurons. J. Neurosci. *25*, 3560–3570.

Rubinson, D.A., Dillon, C.P., Kwiatkowski, A.V., Sievers, C., Yang, L., Kopinja, J., Rooney, D.L., Ihrig, M.M., McManus, M.T., Gertler, F.B., et al. (2003). A lentivirus-based system to functionally silence genes in primary mammalian cells, stem cells and transgenic mice by RNA interference. Nat. Genet. *33*, 401–406.

Sala, C., Piech, V., Wilson, N.R., Passafaro, M., Liu, G., and Sheng, M. (2001). Regulation of dendritic spine morphology and synaptic function by Shank and Homer. Neuron *31*, 115–130.

Salinas, P.C., and Price, S.R. (2005). Cadherins and catenins in synapse development. Curr. Opin. Neurobiol. *15*, 73–80.

Shapiro, L., Fannon, A.M., Kwong, P.D., Thompson, A., Lehmann, M.S., Grubel, G., Legrand, J.F., Als-Nielsen, J., Colman, D.R., and Hendrickson, W.A. (1995). Structural basis of cell-cell adhesion by cadherins. Nature *374*, 327–337.

Stern-Bach, Y., Bettler, B., Hartley, M., Sheppard, P.O., O'Hara, P.J., and Heinemann, S.F. (1994). Agonist selectivity of glutamate receptors is specified by two domains structurally related to bacterial amino acid-binding proteins. Neuron *13*, 1345–1357.

Takeichi, M., and Abe, K. (2005). Synaptic contact dynamics controlled by cadherin and catenins. Trends Cell Biol. *15*, 216–221.

Tamura, K., Shan, W.S., Hendrickson, W.A., Colman, D.R., and Shapiro, L. (1998). Structure-function analysis of cell adhesion by neural (N-) cadherin. Neuron *20*, 1153–1163.

Tanaka, H., Shan, W., Phillips, G.R., Arndt, K., Bozdagi, O., Shapiro, L., Huntley, G.W., Benson, D.L., and Colman, D.R. (2000). Molecular modification of N-cadherin in response to synaptic activity. Neuron *25*, 93–107.

Thoumine, O., Lambert, M., Mege, R.M., and Choquet, D. (2006). Regulation of N-cadherin dynamics at neuronal contacts by ligand binding and cytoskeletal coupling. Mol. Biol. Cell *17*, 862–875.

Togashi, H., Abe, K., Mizoguchi, A., Takaoka, K., Chisaka, O., and Takeichi, M. (2002). Cadherin regulates dendritic spine morphogenesis. Neuron *35*, 77–89.

Uchida, N., Honjo, Y., Johnson, K.R., Wheelock, M.J., and Takeichi, M. (1996). The catenin/cadherin adhesion system is localized in synaptic junctions bordering transmitter release zones. J. Cell Biol. *135*, 767–779.

Wenthold, R.J., Petralia, R.S., Blahos, J.I., and Niedzielski, A.S. (1996). Evidence for multiple AMPA receptor complexes in hippocampal CA1/CA2 neurons. J. Neurosci. *16*, 1982–1989.

Wollmuth, L.P., and Sobolevsky, A.I. (2004). Structure and gating of the glutamate receptor ion channel. Trends Neurosci. *27*, 321–328.

Yap, A.S., Brieher, W.M., Pruschy, M., and Gumbiner, B.M. (1997). Lateral clustering of the adhesive ectodomain: a fundamental determinant of cadherin function. Curr. Biol. *7*, 308–315.

Yu, X., and Malenka, R.C. (2003). Beta-catenin is critical for dendritic morphogenesis. Nat. Neurosci. *6*, 1169–1177.